



Hybrid Nanofluid Flow over a Shrinking Darcy-Forchheimer Porous Medium with Shape Factor and Solar Radiation: A Stability Analysis

Shahirah Abu Bakar^{1,*}, Nurul Syuhada Ismail², Norihan Md Arifin^{3,4}

¹ Takasago Thermal/Engineering Systems Laboratory, Malaysia-Japan International Institute of Technology, Universiti Teknologi Malaysia, 54100, Kuala Lumpur, Malaysia

² Centre for Pre-University Studies, Universiti Malaysia Sarawak, 94300, Kota Samarahan, Sarawak, Malaysia

³ Institute for Mathematical Research, Universiti Putra Malaysia, 43400, UPM Serdang, Selangor, Malaysia

⁴ Department of Mathematics & Statistics, Universiti Putra Malaysia, 43400, UPM Serdang, Selangor, Malaysia

ARTICLE INFO

Article history:

Received 12 July 2023

Received in revised form 15 August 2023

Accepted 18 September 2023

Available online 30 June 2024

Keywords:

Dual solutions; stability analysis; hybrid nanofluid; porous medium; Darcy-Forchheimer; shrinking sheet

ABSTRACT

This research aimed to develop a numerical solution to analyze the effects of solar radiation and nanoparticle shape factors on the flow of a hybrid nanofluid past a shrinking Darcy-Forchheimer porous medium. The base fluid chosen for this study is water (H₂O), and the hybrid nanofluid consists of nanoparticles of silver (Ag) and titanium dioxide (TiO₂) in four different shapes: bricks, cylinders, platelets, and blades. To account for solar radiation, the energy model incorporated a radiative heat flux, while the momentum problem considers the influence of a magnetic field. The application of an appropriate similarity transformation method converts the partial differential equations (PDEs) model into a system of nonlinear ordinary differential equations (ODEs). The mathematical model is solved using the shooting technique method and the *bvp4c* solver. The obtained results, along with the effects of the nanoparticle shape factor, solar radiation parameter, shrinking parameter, Darcy-Forchheimer number, and nanofluid volume fraction, are visually presented through figures and tables. It is worth noting that, in our numerical results, we observed the presence of dual solutions when $\lambda < 0$. Our findings indicate that the thermal transmittance increases with an increase in the nanoparticle shape factor and solar radiative parameter. Additionally, we observed an escalation in the velocity distribution in relation to the shrinking parameter and nanofluid volume fraction. Before reaching the two solutions, a flow stability analysis revealed that the first branch appears to be the most stable. Overall, these findings provide valuable insights into the behaviour of hybrid nanofluid flow in the presence of solar radiation and porous media.

1. Introduction

The wide-ranging applications of heat transfer in engineering, technical, and production industries have always been of great significance, as it directly affects the efficiency of thermal devices. Over the past four decades, numerous studies and research have been conducted to

* Corresponding author.

E-mail address: shahirah.abubakar@utm.my (Shahirah Abu Bakar)

<https://doi.org/10.37934/cfdl.16.11.6081>

enhance the heat transfer rate, with the aim of improving thermal efficiency and achieving energy savings as well as cost reductions in device manufacturing and production [41]. Among the various methods explored, nanofluids were initially introduced by Choi and Eastman [1] in 1995. They dispersed nanoparticles of nanometer size in a base fluid and demonstrated the nanoparticles' ability to enhance thermal transmittance by disrupting nanoscale particles. Building on this, Routbort *et al.*, [2] initiated a project in 2008 to utilize nanofluids for industrial cooling, which aimed to reduce emissions and save energy. The application of nanofluids in heating and cooling water has the potential to save a significant amount of energy in the U.S. industries alone. In the U.S. electric power industry, it has been reported that applying nanofluids in closed-loop cooling cycles could result in a triple joule of energy savings. Furthermore, Wong and Leon [3] stated that this approach could lead to a reduction of approximately 8600 metric tons of NO, 5.6 million metric tons of CO₂, and 21000 metric tons of SO₂ emissions. These findings paved the way for the development of hybrid nanofluids, which involve suspending two different distinct nanoparticles in a fluid. The concept of hybrid nanofluids, as explained by Sarkar *et al.*, [4], aims to further enhance the heat transfer rate and pressure drop characteristics by leveraging the strengths and weaknesses of individual suspensions. Ghadikolaei [5] demonstrated that hybrid nanofluids in fluid flow have the potential to increase the heat transmittance rate due to their favorable aspect ratios and synergistic effects. Aladdin *et al.*, [6] revealed that both mono- and hybrid-nanofluids resulted in a positive increase in the skin friction coefficient, with hybrid nanofluids showing better improvement in shear stress compared to nanofluids alone. Bakar *et al.*, [7] reported a 27.35% increase in heat transfer rate for single-nanofluids and a 36.73% increase for hybrid-nanofluids, indicating a rate increment of 9.38%. Their study also highlighted that an increase in the volume fraction of nanoparticles enhances both solutions of the boundary layer flow, as the shrinking parameter results in the existence of dual solutions. Recent studies on hybrid nanofluid flow have been extensively analyzed by Gul *et al.*, [8], Hussain *et al.*, [9], Lund *et al.*, [10], Muhammad *et al.*, [11], and Rashidi *et al.*, [12].

Renewable energy has gained significant attention in the 21st century due to environmental concerns and the growing demand for energy, including the urgent issue of global warming caused by CO₂ emissions. Among various renewable energy sources, solar energy has emerged as a highly promising option, given its natural abundance as radiation from the Sun. Solar energy is widely regarded as an environmentally friendly, sustainable, and cost-effective source of energy. It requires minimal maintenance and offers a depletion in energy costs. Its applications are vast, ranging from solar power plates, artificial photosynthesis, and solar thermal electricity, as elaborated by Jamshed *et al.*, [13]. Research on solar radiation dates back to 1924, when Angstrom [14] first reported on the topic. Since then, studies on solar radiation have continuously expanded, with recent advancements shedding new light on the subject. Qu *et al.*, [15] demonstrated that even a small concentration of hybrid nanofluid (0.0015%) can significantly enhance the absorption capacity, enabling almost full absorption of solar radiation in the fluid. Acharya [16] examined the thermal patterns of hybrid nanofluid flow within a microchannel under solar radiation. The study revealed temperature augmentation due to solar radiation and hybrid nanofluids, compared to ordinary nanofluids. Alzahrani *et al.*, [17] developed a model for hybrid nanofluid flow through a Darcy-Forchheimer porous medium in the presence of solar radiation. Their findings highlighted the improved efficiency of nanoparticle volume in capturing and transporting solar radiation. Other notable works on hybrid nanofluid flow with solar radiation can be found in the research of Al-Mahmodi *et al.*, [18], Jahan *et al.*, [19], Kumar *et al.*, [20], and Rabbi and Sahin [21]. In conclusion, solar energy has garnered significant attention as a clean and renewable energy source, offering immense potential for addressing environmental concerns and the increasing demand for energy. Ongoing research on solar

radiation and its interaction with hybrid nanofluids contributes to the advancement of solar energy utilization and its integration into various applications.

Porous media is a widely applied technique in various technical and engineering industries due to its large specific surface area and complex pore structure. It finds applications in electronic cooling devices, fuel collectors, and catalytic reactors, packed bed heat exchangers, drying technology devices, and tissue replacement production in biomedical equipment. In the study conducted by Saghir and Rahman [22], four different hybrid nanofluids in a porous media was investigated: MWCNT-Fe₃O₄, Al₂O₃-Cu, TiO₂-SiO₂, and diamond-Fe₃O₄. It was observed that the hybrid MWCNT-Fe₃O₄ nanoparticle mixture exhibited the most promising results among all the combinations. Slimani *et al.*, [23] studied a porous conical system using a hybrid Al₂O₃-Cu/water nanofluid with the presence of a magnetic field. The study indicated that the heat transmittance rate increased with positive values of porosity, Darcy number, and hybrid nanoparticle concentration. Abu Bakar *et al.*, [24] investigated hybrid nanofluid flow over a porous permeable shrinking sheet with slip and radiation, revealing that the parameters considered in their study increased both dual solutions in the skin friction coefficient and velocity distribution. Recent research has further expanded the understanding of hybrid nanofluid flow in porous media, with contributions from Mahn *et al.*, [25], Jino and Kumar [26], Khan *et al.*, [27], Maitra *et al.*, [28], and Shah *et al.*, [29]. Among the various convection flows in porous media, the non-Darcian porous media model is well-known. A modification of Darcian flow, known as the Darcy-Forchheimer model, incorporates the inertia effect in the momentum equation through the velocity squared term, as described by Ganesh *et al.*, [30]. The implementation of fluid flow in Darcy-Forchheimer porous media is of significant importance in mechanical industries, such as insulation design for heat protection, heat pipe construction, cooling of turbine blades, and oil flow filtration. Further studies on this topic have been reported by Gul *et al.*, [31], Khan *et al.*, [32], Ramesh *et al.*, [33], Abu Bakar *et al.*, [34], and Nayan *et al.*, [35].

The particle size and shape factor of nanoparticles play a crucial role in determining the efficiency of heat transfer in fluid flow. The geometry of nanoparticles can be characterized by their shape and size. Nanoparticle properties are influenced by their particle size, with spherical particles being considered the ideal shape. Qi *et al.*, [36] described that the shape factor is defined as the ratio of the surface area of a non-spherical nanoparticle to that of a spherical nanoparticle. Ghadikolaie *et al.*, [37] concluded that platelet-shaped nanoparticles in hybrid TiO₂-Cu/water nanofluid exhibited the highest efficiency compared to cylindrical and brick-shaped nanoparticles. Khan *et al.*, [38] explained that the shape factor directly influenced the temperature field, with blade-shaped nanoparticles performing the best and brick-shaped nanoparticles performing the worst. An analysis of MHD hybrid nanofluid flow inside a porous cavity with nanoparticle shape factor was conducted by Gholinia *et al.*, [39] and they found that lamina-shaped nanoparticles demonstrated the highest Nusselt number, outperforming brick, tetrahedron, and platelet-shaped nanoparticles. Recent studies on hybrid nanofluid flow with nanoparticle shape factor have been conducted by Benkhedda *et al.*, [40], Dinarvand and Rostami [42], Anwar *et al.*, [43], Hafeez *et al.*, [44], Khan *et al.*, [45], Khashi'ie *et al.*, [46], and Rekha Sahoo [47].

In this study, our objective is to investigate the impact of solar radiation and nanoparticle shape factor on the flow of a hybrid nanofluid over a Darcy-Forchheimer porous medium past a permeable shrinking sheet. The mathematical models employed in this work are based on the research conducted by Khan and Alzahrani [48]. The current flow problem is characterized by the inclusion of hybrid nanoparticles, solar radiative heat flux, a permeable surface, a shrinking sheet, and nanoparticle shape factor. For the hybrid nanofluid, we have selected silver (Ag) and titanium dioxide (TiO₂) nanoparticles, with water (H₂O) serving as the base fluid. The combination of Ag- TiO₂ nanoparticles is chosen due to the superior properties of Ag, such as high temperature stability and

corrosion resistance, complemented by the photoactivity efficiency and environmental safety of TiO₂. In addition, this study also explores the influence of non-spherical nanoparticles shapes, including bricks, cylinders, platelets, and blades. These shapes add further complexity to the analysis and enable a comprehensive understanding of the flow behavior. To mathematically model the system, we employ the saturation of the Darcy-Forchheimer relation in the momentum equation. The radiation heat flux is included in the energy equation to consider the effects of solar radiation. Overall, this study aims to contribute to the understanding of the combined effects of solar radiation and nanoparticle shape factor on hybrid nanofluid flow over a Darcy-Forchheimer porous medium where the potential application of this study can be applied in solar collectors, solar stills, or photovoltaic/thermal system and to the best of the authors' knowledge, it is believed that the current problem has never been published anywhere.

2. Mathematical Formulation

2.1 Properties of Fluids and Nanoparticle Shape Factors

This current study deals with hybrid Ag-TiO₂/H₂O nanofluid, where the nanoparticle volume fraction for Ag (φ_1) is selected to be at 5%, while the nanoparticle volume fraction for TiO₂ (φ_2) is chosen to be in the range of $1\% \leq \varphi_2 \leq 5\%$. The volume fraction for hybrid nanofluid is in the form of

$$\varphi_{hmf} = \varphi_1 + \varphi_2 = \frac{V_{Ag} + V_{TiO_2}}{V_{Ag-TiO_2}} \quad [49].$$

To frame the thermophysical properties, we followed the one suggested by Takabi and Salehi [50] and Ghalambaz *et al.*, [51] as listed in Table 1, while Table 2 presented the values of nanoparticles properties and Table 3 demonstrated the size and sphericity of nanoscale particles, which denoted by m .

Table 1

Correlation properties of hybrid nanofluid, see Abu Bakar *et al.*, [34], Takabi and Salehi [50] and Ghalambaz *et al.*, [51]

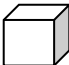
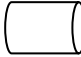

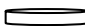
Properties	Hybrid nanofluid correlations
Dynamic viscosity	$\mu_{hmf} = \frac{\mu_f}{(1 - \varphi_1)^{2.5} (1 - \varphi_2)^{2.5}}$
Heat capacity	$(\rho C_p)_{hmf} = (1 - \varphi_2) \left[(1 - \varphi_1) (\rho C_p)_f + \varphi_1 (\rho C_p)_1 \right] + \varphi_2 (\rho C_p)_2$
Density	$\rho_{hmf} = (1 - \varphi_2) \left[(1 - \varphi_1) \rho_f + \varphi_1 \rho_1 \right] + \varphi_2 \rho_2$
Thermal conductivity	$\frac{k_{hmf}}{k_f} = \frac{k_2 + (m-1)k_{nf} - \varphi_2(m-1)(k_{nf} - k_2)}{k_2 + (m-1)k_{nf} + \varphi_2(k_{nf} - k_2)}$ where $\frac{k_{nf}}{k_f} = \frac{k_1 + (m-1)k_{nf} - \varphi_1(m-1)(k_f - k_1)}{k_1 + (m-1)k_f + \varphi_1(k_f - k_1)}$

Table 2

Thermophysical properties for selected nanoparticles, see Dinarvand *et al.*, [52] and Mansourian *et al.*, [53]

Physical properties	Density, ρ (kg/m ³)	Specific heat, C_p (J/kg K)	Thermal conductivity, k (W/m K)
Water	997.1	4179	0.613
Ag	10500	235	429
TiO ₂	4250	686	8.9538

Table 3
 Shape, size, and geometrical appearance for a nanoparticle, see Gholinia *et al.*, [39]

Shape	Size	Geometrical schematic
Bricks	3.7	
Cylinders	4.9	
Platelets	5.7	
Blades	8.6	

2.2 Mathematical Modelling

In this study, we consider a 2D steady flow of hybrid – nanofluid over a permeable shrinking surface of porous medium in presence of solar radiation and nanoparticle shape factor as illustrated in Figure 1. The porous space is saturated by an incompressible liquid that characterize the relationship of Darcy-Forchheimer. The surface velocity is deformed by $U_w(x) = cx$ where c is the coefficient of the plate velocity and described by $c > 0$ for stretching plate while $c < 0$ is shrinking plate. The dispersion of the nanoparticles in the base fluid is assumed to be in a state of thermal equilibrium, together with the temperature of the fluid below the sheet is T_f and the ambient temperature is T_∞ . The desired governing equations are extended by Khan and Alzahrani [49] by including the above assumption which can be written by

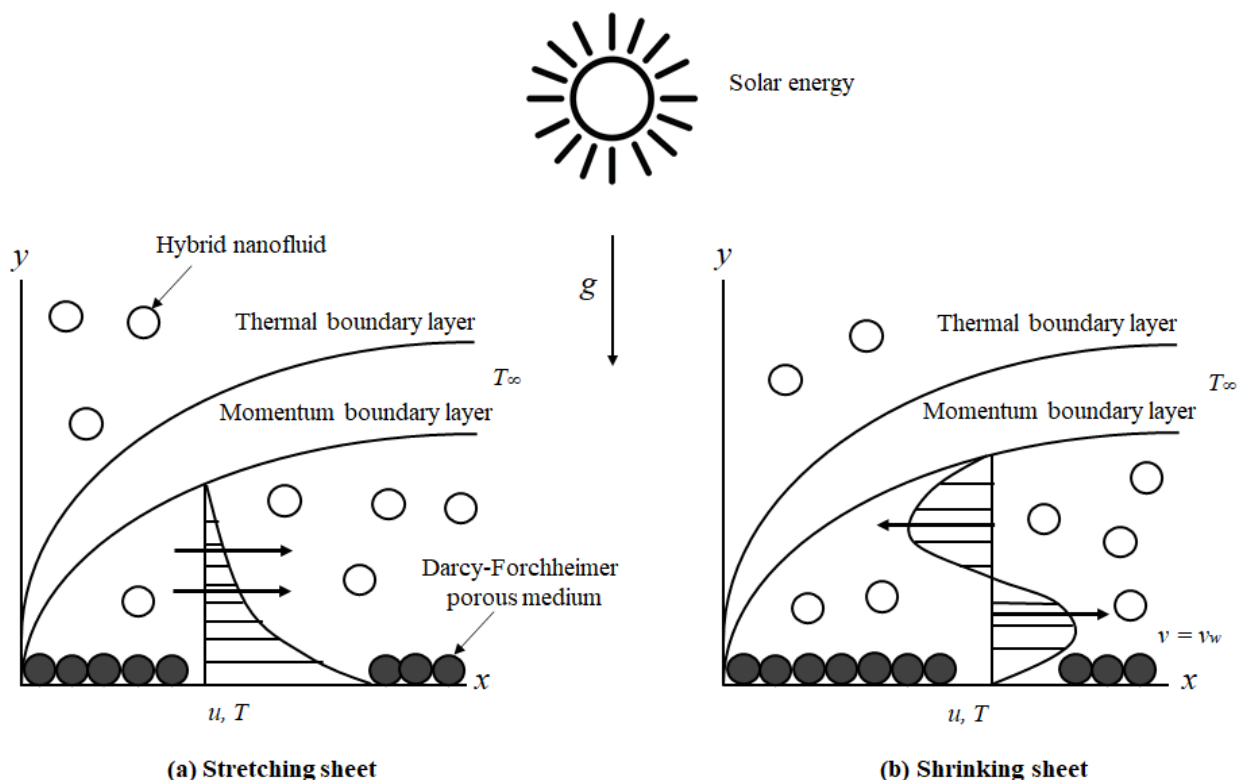


Fig. 1. Schematic diagram of current problem

$$\frac{\partial u}{\partial x} + \frac{\partial v}{\partial y} = 0 \quad (1)$$

$$u \frac{\partial u}{\partial x} + v \frac{\partial u}{\partial y} = \frac{\mu_{hmf}}{\rho_{hmf}} \frac{\partial^2 u}{\partial y^2} - \frac{\mu_{hmf}}{\rho_{hmf}} \frac{u}{K^*} - \frac{\sigma_{hmf} B_0^2}{\rho_{hmf}} u - F_c u^2 \quad (2)$$

$$u \frac{\partial T}{\partial x} + v \frac{\partial T}{\partial y} = \frac{k_{hmf}}{(\rho C_p)_{hmf}} \frac{\partial^2 T}{\partial y^2} - \frac{1}{(\rho C_p)_{hmf}} \frac{16\sigma^* T^3}{3K^*} \frac{\partial^2 T}{\partial y^2} \quad (3)$$

With the boundary conditions at

$$\begin{aligned} u = U_w(x), v = v_w(x), T = T_w \text{ as } y \rightarrow 0 \\ u \rightarrow 0, T \rightarrow T_\infty \text{ at } y \rightarrow \infty \end{aligned} \quad (4)$$

Here u and v are the velocities of x - and y -axis while T is temperature. The final expression in Eq. (3) represents the non-linear radiative of solar energy where σ^* is the Stefan-Boltzmann constant and K^* is the mean absorption coefficient. Further, B_0 is the strength of magnetic field,

$F_c = \frac{C_b}{x\sqrt{K^*}}$ is the non-uniform inertia coefficient where C_b is the drag force coefficient, while ρ_{hmf} , μ_{hmf} , k_{hmf} , $(\rho C_p)_{hmf}$ and σ_{hmf} represent density, dynamic viscosity, thermal conductivity, specific heat and electrical conductivity of hybrid Nano-suspension, accordingly.

We now introduce the similarity variables as follows, see Khan and Alzahrani [48]

$$u = cx f'(\eta), v = -\sqrt{cv_f} f(\eta), \theta = \frac{T - T_\infty}{T_w - T_\infty}, \eta = y \sqrt{\frac{c}{v_f}} \quad (5)$$

Where Eq. (1) is satisfied, while Eq. (2) and Eq. (3) can deduce to

$$\frac{1}{A_1 A_2} (f''' - Kf') - \frac{M^2}{A_2} f' + ff'' - (f')^2 (D_f + 1) = 0 \quad (6)$$

$$(A_3 + N)\theta'' + A_4 Pr f\theta' = 0 \quad (7)$$

Pertaining to the boundary conditions at

$$\begin{aligned} f(0) = S, f'(0) = \lambda, \theta'(0) = 1 \text{ when } \eta = 0 \\ f'(\eta) \rightarrow 0, \theta(\eta) \rightarrow 0 \text{ as } \eta \rightarrow \infty \end{aligned} \quad (8)$$

When K , M , D_f , N , Pr and S are porous medium permeability, magnetic parameter, inertia coefficient or Darcy-Forchheimer number, solar radiation parameter, Prandtl number and suction parameter, correspondingly, which are mathematically described by

$$K = \frac{\mu_f}{\rho_f c K^*}, M = \frac{\sigma_f B_0^2 c}{\mu_f}, D_f = \frac{C_b}{\sqrt{K^*}}, N = \frac{16 \sigma^* T_\infty^3}{3 k^* k}, \text{Pr} = \frac{\nu_f}{\alpha_f}, S = -\frac{v_w}{\sqrt{c \nu_f}},$$

$$A_1 = (1 - \varphi_2) \left(1 - \varphi_1 + \frac{\varphi_1 \rho_1}{\rho_f} \right) + \frac{\varphi_2 \rho_2}{\rho_f}, A_2 = (1 - \varphi_1)^{2.5} (1 - \varphi_2)^{2.5}, A_3 = \frac{k_{hmf}}{k_f},$$

$$A_4 = (1 - \varphi_2) \left(1 - \varphi_1 + \frac{\varphi_1 (\rho C_p)_1}{(\rho C_p)_f} \right) + \frac{\varphi_2 (\rho C_p)_2}{(\rho C_p)_f}.$$

Physical quantities of interest that convey the essential data for engineers to design apparatus by utilizing hybrid nanoparticles are the coefficient of skin friction C_f and Nusselt number Nu_x . Following Aly and Pop [54], these quantities are assumed to be frame at the lower surface of the plate and can be written in the form of

$$C_f = \frac{\tau_w}{\rho_f U_w^2}, Nu_x = \frac{x q_w}{k_f (T_w - T_\infty)} \quad (10)$$

Where $\tau_w = -\mu_{hmf} \frac{\partial u}{\partial y} \Big|_{y=0}$ and $q_w = -k_{hmf} \frac{\partial T}{\partial y} \Big|_{y=0}$ are shear stress along the plate and heat flux from the plate, accordingly. By employing the similarity variables in Eq. (5), the reduced form of C_f and Nu_x are finalized by

$$C_f \sqrt{\text{Re}_x} = \frac{1}{A_2} f''(0), Nu_x \sqrt{\frac{1}{\text{Re}_x}} = -(A_3 + N) \theta'(0) \quad (11)$$

Where $\text{Re}_x = \frac{U_w(x)x}{\nu_f}$ is Reynolds number.

2.3 Procedure of Numerical Approach

The non-linear ordinary differential equations ODEs presented in Eq. (6) and Eq. (7), along with the corresponding boundary conditions in Eq. (8), are solved numerically using the shooting technique method implemented in MAPLE software. The shooting technique method is commonly employed in numerical analysis to transform a boundary value problem (BVP) into an initial value problem (IVP). This transformation involves “shooting” trajectories in various directions until the desired trajectory is obtained, which satisfies the BVP, see Bakar *et al.*, [7]. To solve the higher-order ODEs described in Eq. (6) and Eq. (7), they are first converted into code form and subsequently executed as an IVP. In this process, the variables are labelled as follows

$$f = y_1, f' = y_1' = y_2, f'' = y_2' = y_3,$$

$$\theta = y_4, \theta' = y_4' = y_5.$$

Hence, the ODEs in Eq. (6) and Eq. (7) are then formulated into

$$\begin{pmatrix} y_1' \\ y_2' \\ y_3' \\ y_4' \\ y_5' \end{pmatrix} = \begin{pmatrix} y_2 \\ y_3 \\ (K + A_1 M^2) y_2 - A_1 A_2 y_1 y_3 + A_1 A_2 (y_2)^2 (D_f + 1) \\ y_5 \\ -\frac{A_4 Pr y_1 y_5}{A_3 + N} \end{pmatrix}.$$

Initially, the values are selective to be guessed when the initial conditions are not given. In condition of $\eta \rightarrow \infty$ at each parameter, the end of boundary layer region is determined when the unknown boundary layer values are fixed with the consecutive iterative step length is less than 10^{-7} .

3. Results and Discussions

Before discussing the mathematical models presented in Eq. (6) – Eq. (8), a comparison was conducted between the current results and the findings of Khan and Alzahrani [48] and Gorla and Sidawi [55], as outlined in Table 4. The comparison reveals a strong consensus and agreement between the different studies, with additional distinct outcomes that can be identified accordingly. In Figure 2, the stream flows for two different numbers of Ag-nanoparticle φ_1 are illustrated. It can be observed that the flow rate becomes constrained or restricted in the central region due to the meandering nature of the fluid flow. This phenomenon occurs because the nanoparticles experience more collisions with the meandering surface, leading to a decrease in flow rate.

Table 4
 Comparison of $-\theta'(0)$ against Pr when $\lambda = 1.0$

Pr	$-\theta'(0)$		
	Khan and Alzahrani [48]	Gorla and Sidawi [55]	Present outcomes
0.2	0.1688	0.16912	0.1688237
0.7	0.4579	0.53488	0.4539061
2.0	0.9119	0.91142	0.9113576
3.0	-	1.15970	1.1596994
7.0	1.8994	1.89046	1.8984302
10.0	-	2.30350	2.3139646
20.0	3.3539	3.35391	3.3539049

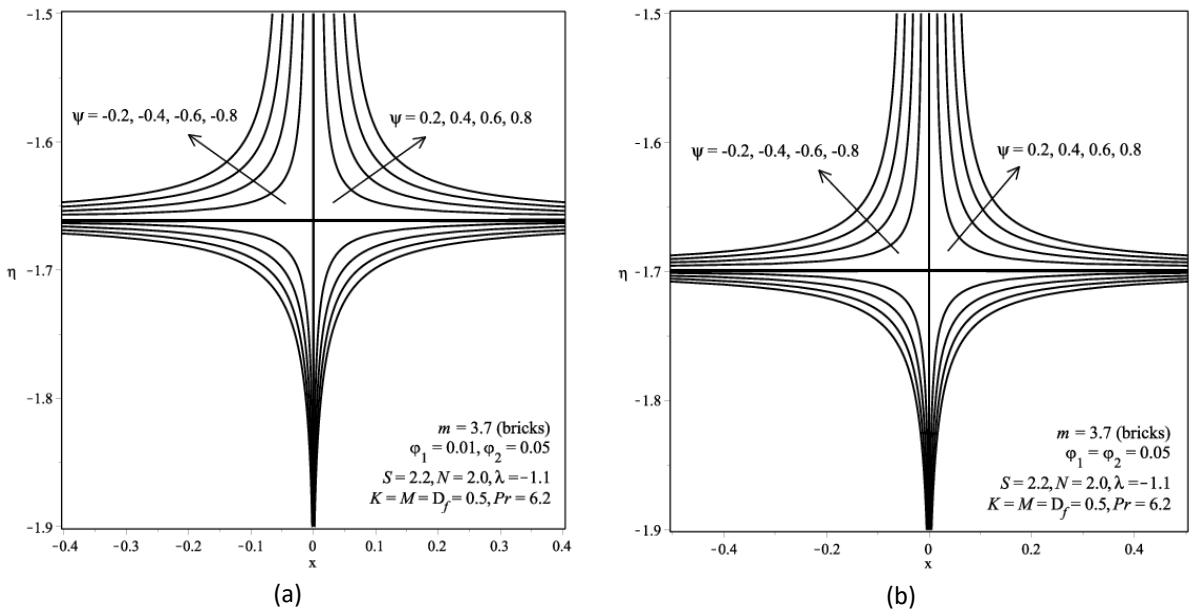
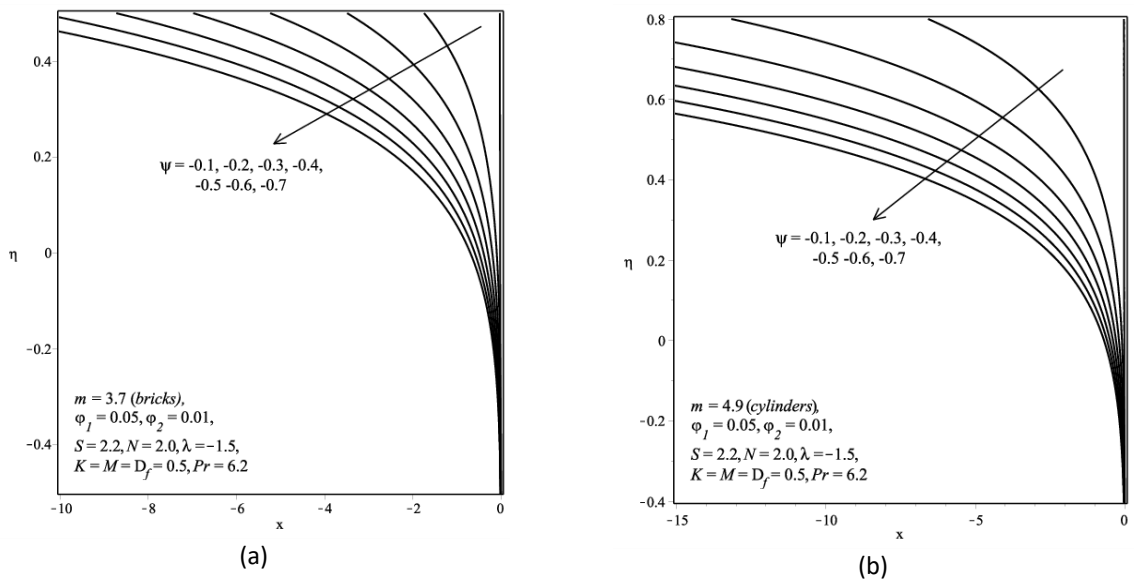


Fig. 2. Streamline flows for (a) Hybrid nanofluid of $\phi_1 = 0.01$ and $\phi_2 = 0.05$ (b) Hybrid nanofluid of $\phi_1 = \phi_2 = 0.05$

Further, Figure 3 presents the streamline flows of four different nanoparticle shapes m . It can be observed that as the value of m increases, the streamline flows become more predominantly laminar. In Figures 4(a) and 4(b), the impact of TiO_2 -nanoparticles ϕ_2 on the skin friction coefficient $f''(0)$ and temperature gradient $-\theta'(0)$ with respect to the shrinking parameter is illustrated. Within the range of $\lambda_c \leq \lambda < 0$, a non-unique solution is observed. This non-unique solution causes the bifurcation of branches, resulting in two solutions known as the first and second solutions (or first and second branches). The critical value of the solution, denoted as λ_c , corresponds to the peak of this bifurcation. In Figure 4, it is evident that both fluid flow and heat transfer rate exhibit significant expansion with increasing value of ϕ_2 . This increment indicates that the volumetric fraction of nanoparticles is pressed towards the wall direction as the viscosity of the buoyancy forces increases.



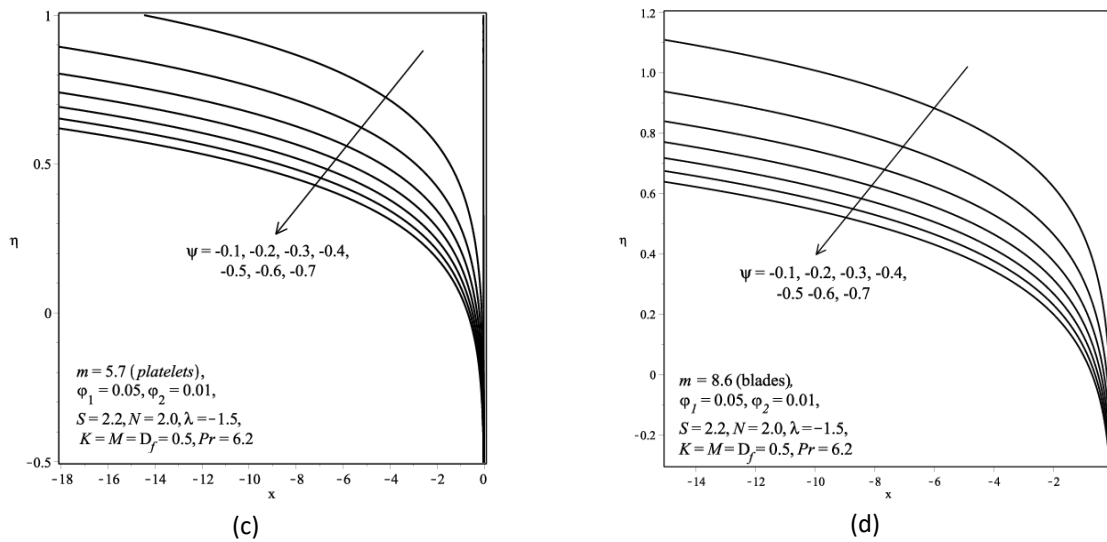


Fig. 3. Streamline flows for nanoparticle shape factor m when (a) $m = 3.7$ (bricks-shaped) (b) $m = 4.9$ (cylinders-shaped) (c) $m = 5.7$ (platelets-shaped) (d) $m = 8.6$ (blades-shaped)

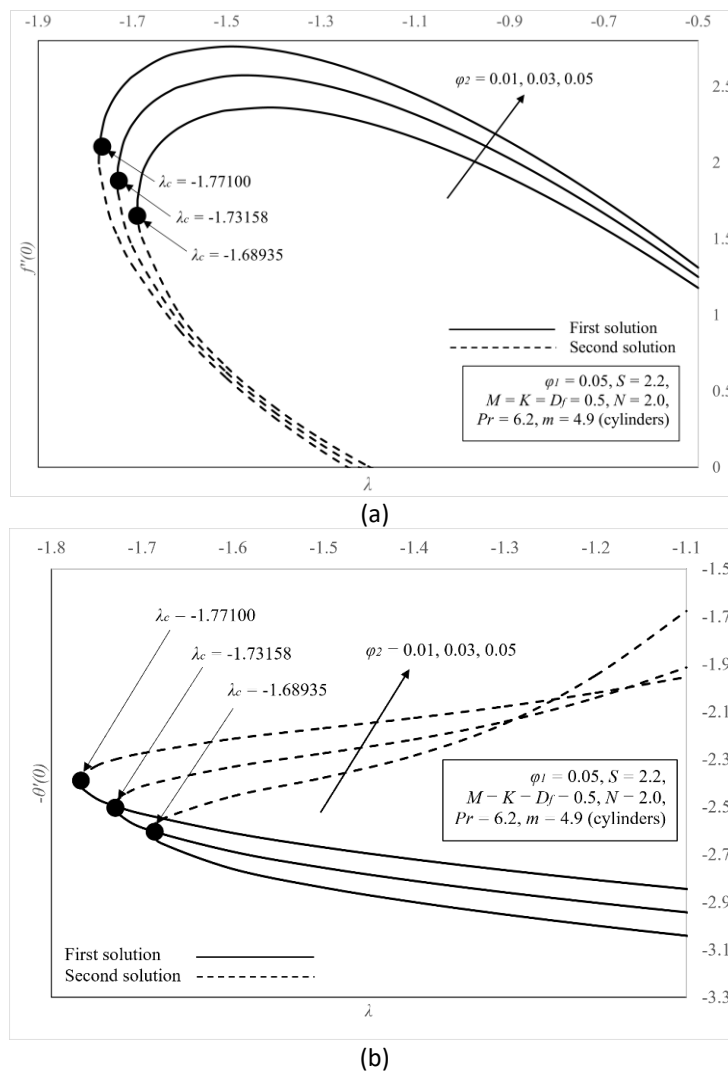


Fig. 4. Influence of ϕ_2 on (a) Skin friction coefficient $f''(0)$ (b) Temperature gradient $-\theta'(0)$

The effect of Darcy-Forchheimer number or inertia coefficient parameter D_f on $f''(0)$ and $-\theta'(0)$ is illustrated in Figures 5(a) and 5(b), respectively. From both figures, a significant increment pattern is noticed when D_f expanded from 0.3 to 1.0. Inertia coefficient can be described by the ability of mass to resist a transition, where any additional amount of D_f may expand the resistance and produce a strong movement in the fluid flow. This reaction subsequently enhances both flows in $f''(0)$ and $-\theta'(0)$. Figures 6(a) and 6(b) presented the impact of solar radiation parameter N and nanoparticle shape factor m on $-\theta'(0)$ against λ , accordingly. From Figure 6(a), it is noticed that the heat transmittance escalates as N increases, which can be explained by the increasing amount of mean absorption coefficient resulting in more amount of heat transfer rate. Simultaneously, the pattern of increment in Figure 6(b) justifies that the temperature is at the highest for $m = 8.6$ (blades-shaped) and the lowest is for $m = 3.7$ (bricks-shaped).

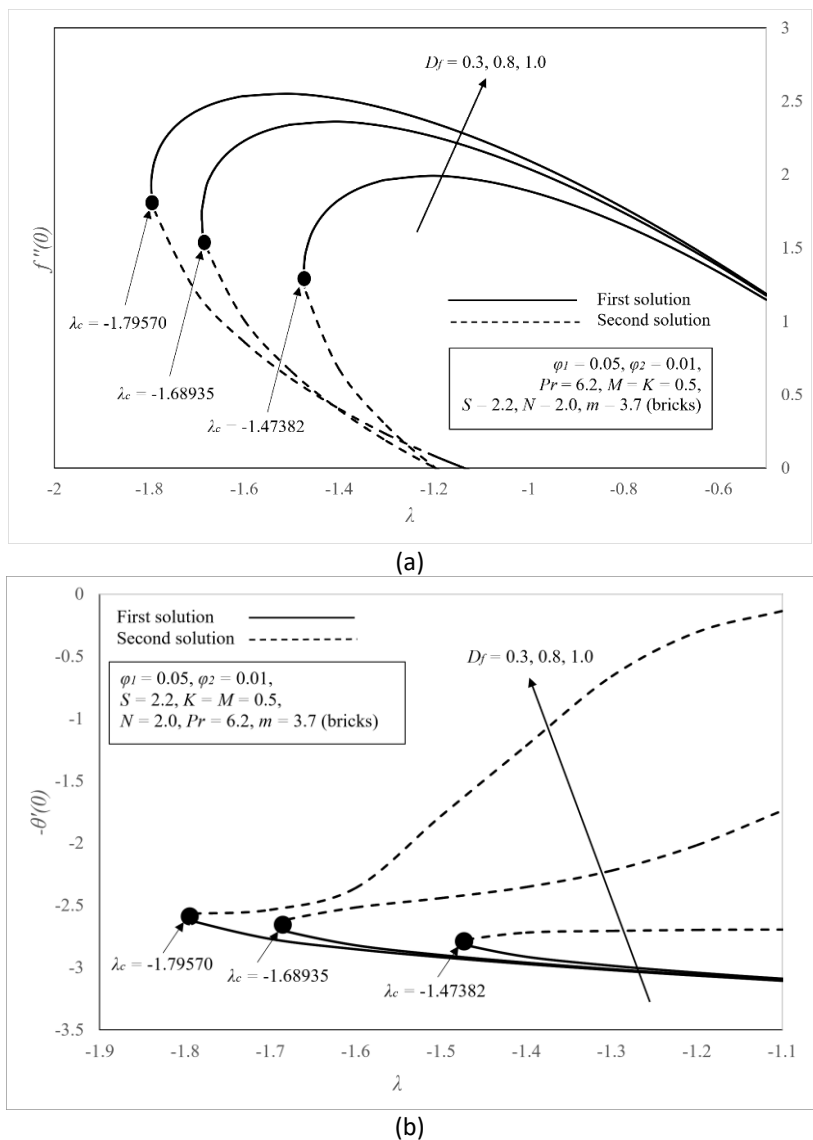


Fig. 5. Influence of D_f on (a) Skin friction coefficient $f''(0)$ (b) Temperature gradient $-\theta'(0)$

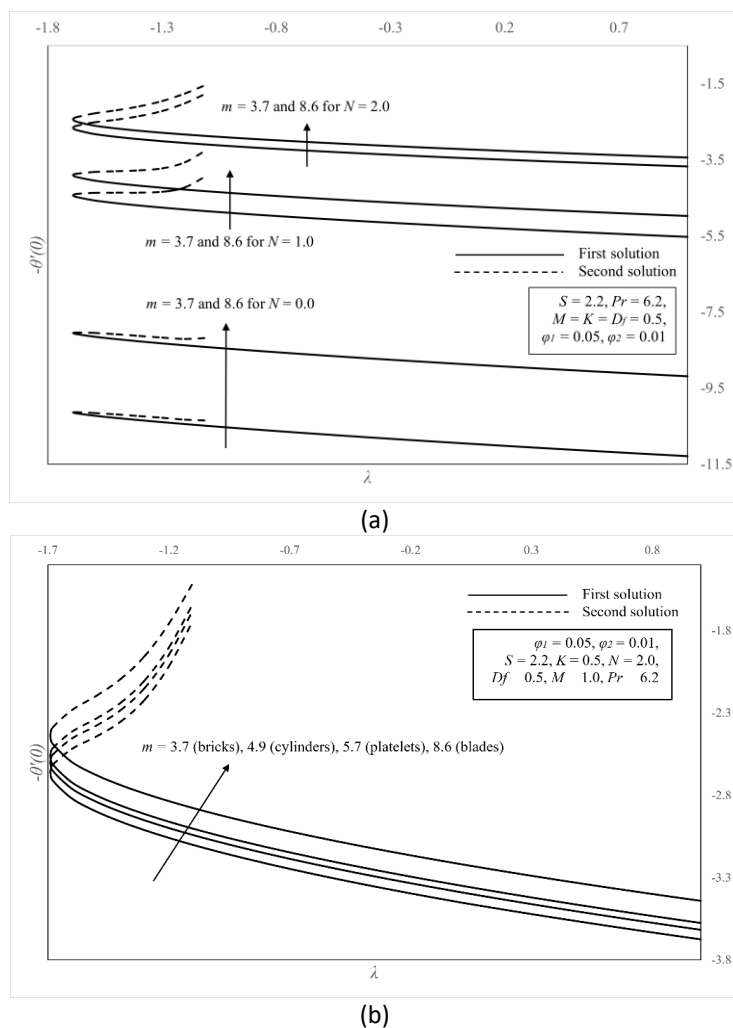


Fig. 6. Temperature gradient $-\theta'(0)$ against (a) Numbers of N
 (b) Numbers of m

The velocity and temperature profiles exhibit overall enhancements, as shown in Figures 7(a) and 7(b), respectively, in relation to the TiO_2 - nanoparticles φ_2 , except for a decline observed in the second solution of the velocity profiles. Physically, the introduction of an increasing φ_2 triggers the development of viscous forces within the nanofluid which resistance arises among the fluid particles, leading to an increase in heat transfer rate within the temperature profiles $\theta(\eta)$, while simultaneously causing a decrease in fluid particle velocity. Figures 8(a) and 8(b) convey the impact of shrinking parameter λ on the dimensionless profiles of velocity $f'(\eta)$ and temperature $\theta(\eta)$, accordingly. A brief observation can be made that the lowest temperature in the first branch is conceived prior to the highest number of λ , while the other solutions in both profiles possessed an improvement. This can be explained due to the hybridity in the shrinking surface boosting the velocity distribution but dragged away the first branch of heat transfer rate.

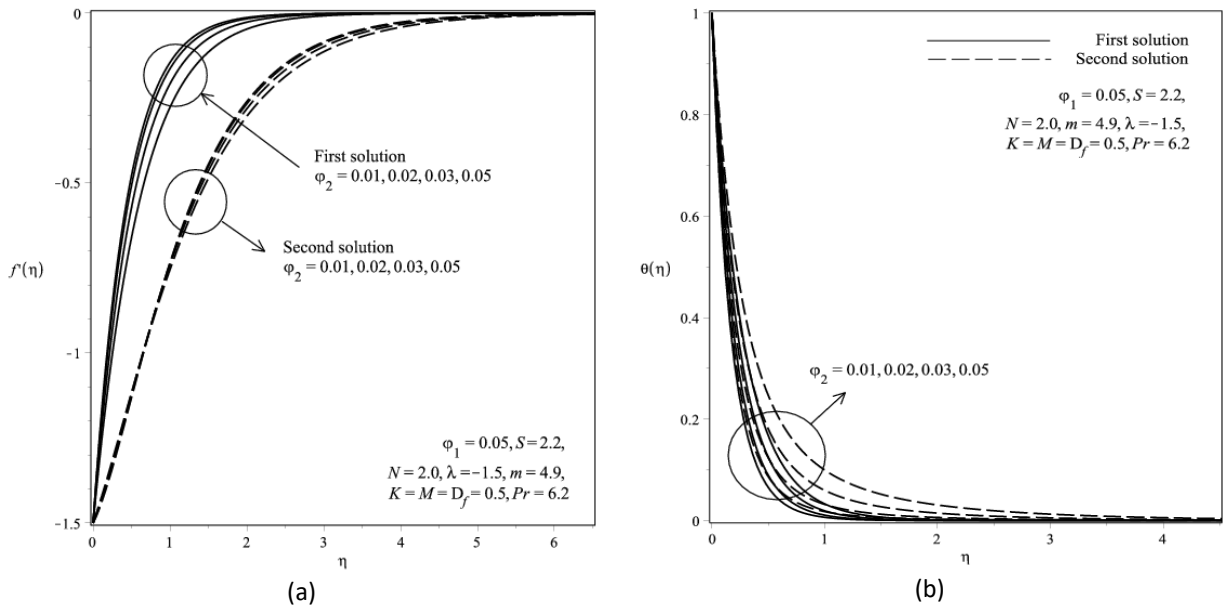


Fig. 7. Numbers of TiO_2 -nanoparticles ϕ_2 against (a) Velocity profiles $f'(\eta)$ (b) Temperature profiles $\theta(\eta)$

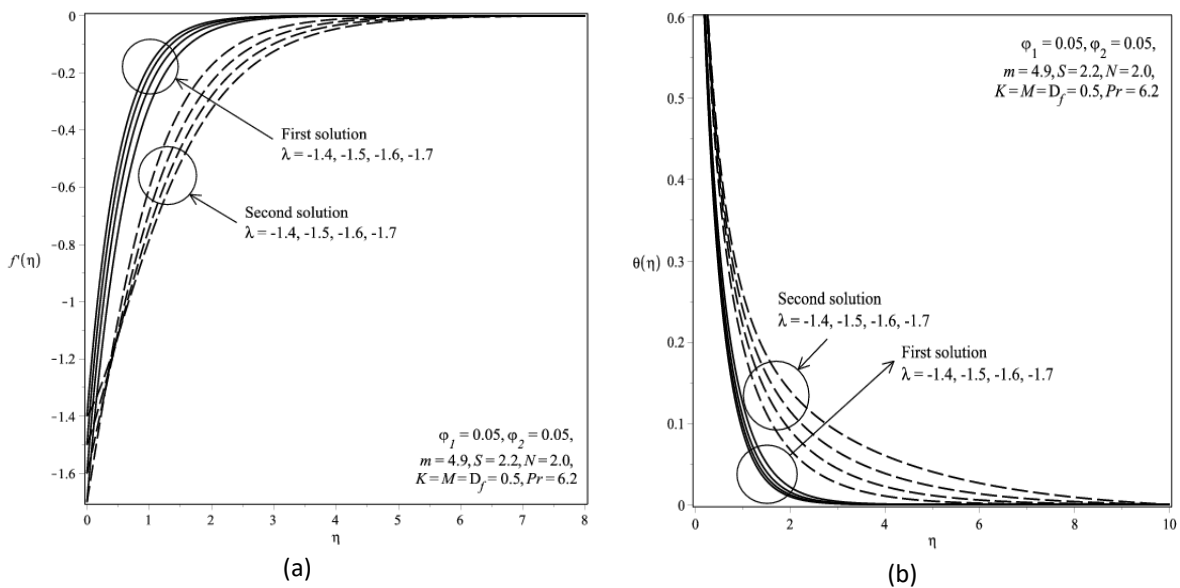


Fig. 8. Numbers of shrinking parameter λ against (a) Velocity profiles $f'(\eta)$ (b) Temperature profiles $\theta(\eta)$

The dimensionless temperature profiles $\theta(\eta)$ for hybrid nanofluid flow with selected number of nanoparticle shape factor m and solar radiation parameter N are distributed in Figures 9(a) and 9(b), respectively. Here, velocity profiles $f'(\eta)$ for m and N are not included due to the influence of these factors are directly proportion to temperature distribution while velocity distribution remains unchanged. From Figure 9(a), blades-shaped nanoparticle ($m = 8.6$) possessed the highest heat transfer rate in both branches of solutions, followed by platelets-shaped, cylinders-shaped and bricks-shaped. Based on the Figure 9(b), a dual pattern is distinguished against the factor of N , where this can be explained by the reducing amount of mean absorption coefficient when there is an increment in N , which resulting in less amount of heat transfer rate. Simultaneously, the increment of first solution in Figure 9(b) can be described by each additional number of N by releasing a

sufficient heat energy in the system and this possessed the domination of radiation over conduction in the fluid flow, where the transfer rate of solar radiation was measured by the amplification of $\frac{16 \sigma^* T_\infty^3}{3 K^* k}$ in N factor. Further, Figure 10 employed the decrement of boundary layer thickness for hybrid nanofluid solutions when the intensity of the magnetic field parameter M increases. Magnetic field creates a resistance of Lorentz force that works best in depreciate the velocity in fluid flow and thus acknowledged the definition of declining patterns in both solutions.

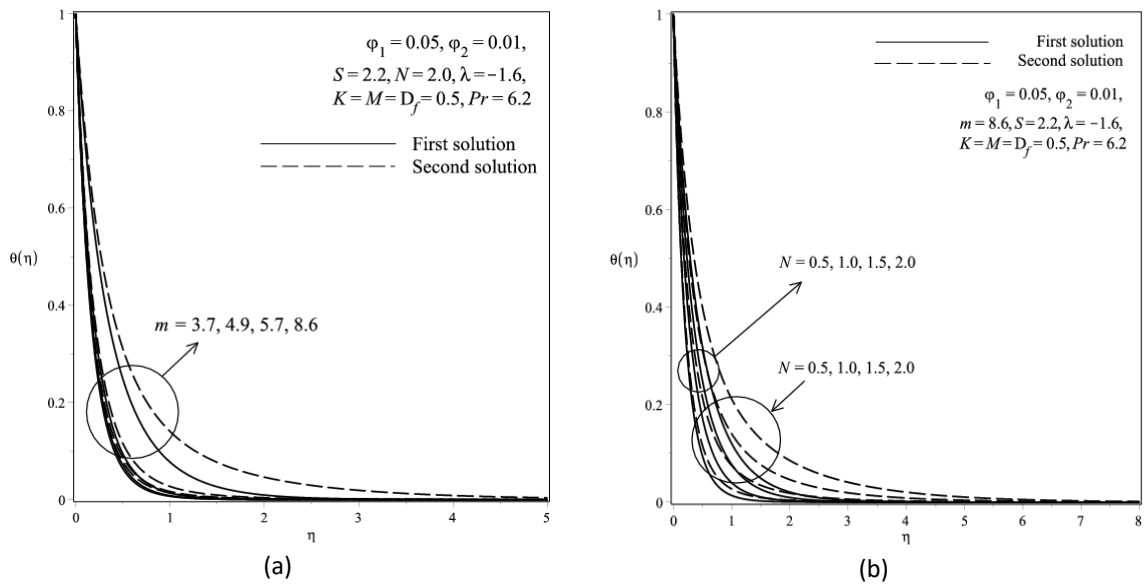


Fig. 9. Temperature profiles $\theta(\eta)$ against (a) Numbers of m (b) Numbers of N

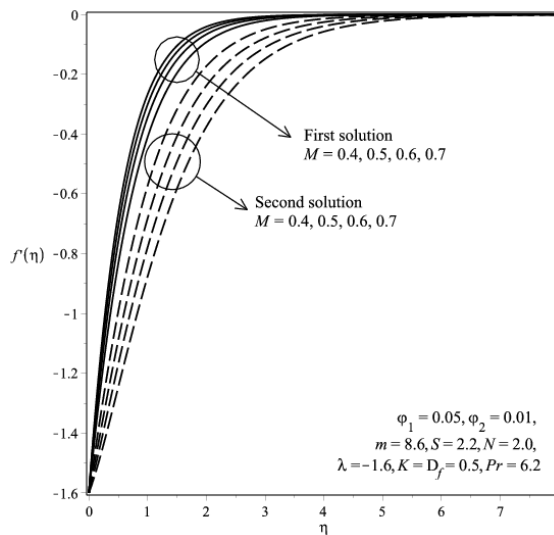


Fig. 10. Velocity profiles $f'(\eta)$ against M

Figure 11 then presented the percentage of heat transmittance rate within the mono- and hybrid-nanofluids flow when $Ag-\varphi_1 = 5\%$ and $0\% \leq TiO_2 - \varphi_2 \leq 5\%$. Here, it is clearly observed that the heat transfer rate for mono-nanofluid (Ag/water nanoparticle) is 42.93%, while the highest rate is 58.29% perceived by hybrid-nanofluid (5% of Ag, 5% of TiO_2). This indicating that the heat transfer rate conceived better performance by hybrid-nanofluid volume fraction compared to mono-nanofluid with the gap of 15.36%.

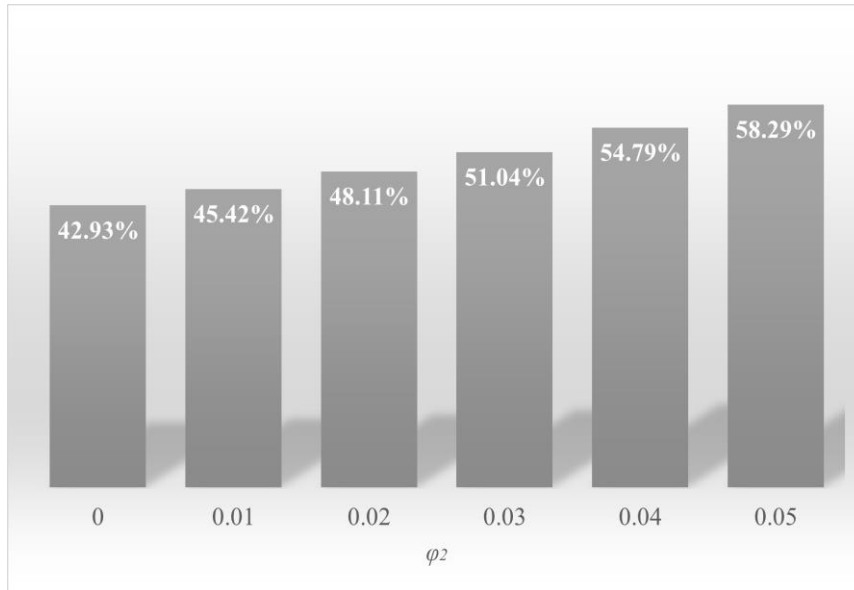


Fig. 11. Heat transfer rate for mono- and hybrid-nanofluids

4. Stability Analysis

Stability analysis is performed in this study as to differentiate the realizable physical solution between two branches of solutions possessed by shrinking parameter λ , as emphasized by Ismail *et al.*, [56] and Ismail *et al.*, [57]. To analyse such condition, Weidman *et al.*, [58] and Merkin [59] suggested to imply Eq. (2) – Eq. (4) in an unsteady condition while Eq. (1) is being held. Prior to this, a new dimensionless time variable in the form of τ is also introduced with the similarity variables in Eq. (5)

$$u = cx f'(\eta), v = -\sqrt{cv_f} f(\eta), \theta = \frac{T - T_\infty}{T_w - T_\infty}, \eta = y \sqrt{\frac{c}{\nu_f}}, \tau = ct \quad (12)$$

Where t represents time. The unsteadiness flow may be due to natural processes since the flow in any situations is relying on time, and it is more complex than the steady flows as the conditions of unsteady flow vary with respect to time and space, as explained by Abu Bakar *et al.*, [34]. Thus, with the consideration of our unsteady mathematical models and Eq. (12), we have

$$\frac{1}{A_1 A_2} \left(\frac{\partial^3 f}{\partial \eta^3} - K \frac{\partial f}{\partial \eta} \right) - \frac{M^2}{A_2} \frac{\partial f}{\partial \eta} + f \frac{\partial^2 f}{\partial \eta^2} - \left(\frac{\partial f}{\partial \eta} \right)^2 (D_f + 1) - \frac{\partial^2 f}{\partial \tau \partial \eta} = 0 \quad (13)$$

$$(A_3 + N) \frac{\partial^2 \theta}{\partial \eta^2} + A_4 \text{Pr} f \frac{\partial \theta}{\partial \eta} - \frac{\partial \theta}{\partial \tau} = 0 \quad (14)$$

With the boundary conditions at

$$f(0, \tau) = S, \quad \frac{\partial f(0, \tau)}{\partial \eta} = \lambda, \quad \theta(0, \tau) = 1 \text{ at } \eta = 0$$

$$\frac{\partial f(\tau, \eta)}{\partial \eta} \rightarrow 0, \quad \theta(\tau, \eta) \rightarrow 0 \text{ as } \eta \rightarrow \infty$$
(15)

Weidman *et al.*, [58] and Merkin [59] then proposed the stability flow analysis as

$$f(\eta, \tau) = f_0(\eta) + e^{-\beta\tau} F(\eta), \quad \theta(\eta, \tau) = \theta_0(\eta) + e^{-\beta\tau} G(\eta)$$
(16)

Here, f_0 and θ_0 are the small relatives of $F(\eta)$ and $G(\eta)$, accordingly, and β is the unknown eigenvalue parameter that represents the expansion or deterioration of a disturbance rate. Eigenvalues can be used to determine whether a fixed point is stable or not stable such that a system can be initially disturbed around its fixed point and yet eventually return to its original location and remain there, see Abu Bakar *et al.*, [60], Bakar *et al.*, [61] and Ismail *et al.*, [62]. The solution of eigenvalues provides an infinite set of $\beta_1 < \beta_2 < \beta_3 < \dots$, where the negative or positive numbers of β represent the rate of expansion or deterioration of a disturbance rate. For instance, a negative number of β indicated that the disturbance rate is expanded, and the solution is unstable; and vice versa.

Further, the following linearized equations are obtained by adopting Eq. (16) into Eq. (13) – Eq. (15).

$$\frac{1}{A_1 A_2} (F''' - KF') - \frac{M^2}{A_2} F' + f_0 F'' + f_0'' F - 2f_0' F' (D_f + 1) + \beta F' = 0$$
(17)

$$(A_3 + N)G'' + A_2 \text{Pr}(\theta_0' F + f_0 G' + \beta G) = 0$$
(18)

Prior to the boundary conditions at

$$F(\eta) = 0, \quad F'(\eta) = 0, \quad G(\eta) = 0 \text{ at } \eta = 0$$

$$F'(\eta) \rightarrow 0, \quad G(\eta) \rightarrow 0 \text{ as } \eta \rightarrow \infty$$
(19)

Following Harris *et al.*, [63], the condition of $F'(\eta) \rightarrow 0$ is putted at rest and replaced with the condition of $F''(\eta) = 1$ as $\eta \rightarrow \infty$. Hence, Table 5 listed the smallest eigenvalue β versus two different amounts of hybrid nanoparticles volume fraction, while the list of β number series against Darcy-Forchheimer number D_f and suction parameter S are presented in Tables 6 and 7, respectively. A series of positive amounts are observed in all first branch of solution, while the second branch of solution is distinguished to be in a series of negative numbers as can be noticed in these three tables. Thus, from the definition of eigenvalue β , a firm conclusion can be drawn as the first branch is stable and the other solution is contrariwise.

Table 5
 Different amounts of hybrid nanoparticles and smallest eigenvalue β

φ_1	φ_2	λ	β	
			First branch of solution	Second branch of solution
5%	1%	-1.2	0.00347	-0.00995
		-1.3	0.01058	-0.01584
		-1.4	0.14309	-0.14773
	5%	-1.2	0.01149	-0.01092
		-1.3	0.16873	-0.02961
		-1.4	0.30908	-0.15089

Consideration of $m = 3.7, S = 2.2, N = 2.0, K = M = D_f = 0.5$ and $Pr = 6.2$

Table 6
 Darcy-Forchheimer number D_f and smallest eigenvalue β

D_f	λ	β	
		First branch of solution	Second branch of solution
0.5	-1.4	0.30908	-0.15089
	-1.5	0.37334	-0.29055
1.0	-1.4	0.36211	-0.43783
	-1.5	0.40918	-0.47720

Consideration of $\varphi_1 = \varphi_2 = 0.05, m = 3.7, S = 2.2, N = 2.0, K = M = 0.5$ and $Pr = 6.2$

Table 7
 Suction parameter S and smallest eigenvalue β

S	λ	β	
		First branch of solution	Second branch of solution
3.0	-1.4	0.40132	-0.26269
	-1.5	0.45339	-0.39730
4.0	-1.4	0.58297	-0.35521
	-1.5	0.63189	-0.44560

Consideration of $\varphi_1 = \varphi_2 = 0.05, m = 3.7, N = 2.0, K = M = D_f = 0.5$ and $Pr = 6.2$

5. Conclusions

In this study, we investigate a steady, 2D flow of a hybrid – nanofluid over a magnetic shrinking surface filled with a Darcy-Forchheimer porous medium and exposed to solar radiation. The hybrid nanofluid is formed by dispersing two types of nanoparticles, Ag and TiO₂, in water. To analyze the flow behavior, a system of ODEs is derived from the non-linear PDEs using the similarity transformation method. These ODEs are then solved using the shooting technique method in MAPLE software and the bvp4c solver in MATLAB software. The current study examines the impact of various parameters on the flow field, including the nanoparticle volume fraction φ , shrinking parameter λ , solar radiation parameter N , Darcy-Forchheimer number D_f , nanoparticle shape factor m and magnetic field parameter M . It is found that these parameters have significant effects on the flow characteristics based on the following outcomes

- i) Two branches of solutions are possessed prior to the shrinking surface $\lambda < 0$.

- ii) The range of λ_c is significantly expanded as the number of φ_2 and D_f increase.
- iii) Heat transfer rate showed a significant improvement by hybrid nanofluid compared to mono nanofluid with the difference of 15.36%.
- iv) Velocity and temperature profiles are directly overcome with nanoparticle volume fraction φ , nanoparticle shape factor m , shrinking parameter λ , Darcy-Forchheimer number D_f and solar radiation parameter N , while magnetic field parameter M divert the pattern.
- v) Blades-shaped nanoparticles possessed the highest heat transfer rate in both branches of solutions, followed by platelets-shaped, cylinders-shaped, and bricks-shaped.
- vi) Stability analysis is performed on the mathematical model due to dual solutions, and the first branch showed the most stable compared to the second branch.

In conclusion, this work offers valuable insights into the behavior of hybrid nanofluid flow over a magnetic shrinking surface within a Darcy-Forchheimer porous medium under solar radiation. These findings contribute to a deeper understanding of the flow field and its dependence on the considered parameters. It is also anticipated that the results obtained from this study will be beneficial to academicians and researchers in the same field.

Statement and Declarations

The authors declare that there are no conflict of interest or personal relationship were reported in this work.

Acknowledgement

The authors would like to express their appreciation to Takasago Engineering Co. Ltd. through the grant number 4B732, as well as to Universiti Teknologi Malaysia (UTM), Universiti Malaysia Sarawak (UNIMAS), Universiti Putra Malaysia (UPM) and Ministry of Higher Education Malaysia (MOHE).

Author Contributions

S.A.B. and N.S.I. developed the flow model, performed computational analysis, and wrote the paper, while N.M.A. validated the computational analysis and numerical results.

References

- [1] Choi, S. US, and Jeffrey A. Eastman. *Enhancing thermal conductivity of fluids with nanoparticles*. No. ANL/MSD/CP-84938; CONF-951135-29. Argonne National Lab.(ANL), Argonne, IL (United States), 1995.
- [2] Routbort, J. "Argonne national lab, michellin north america, st." *Gobain Corp* (2009).
- [3] Wong, Kaufui V., and Omar De Leon. "Applications of nanofluids: current and future." *Advances in mechanical engineering* 2 (2010): 519659. <https://doi.org/10.1155%2F2010%2F519659>
- [4] Sarkar, Jahar, Pradyumna Ghosh, and Arjumand Adil. "A review on hybrid nanofluids: recent research, development and applications." *Renewable and Sustainable Energy Reviews* 43 (2015): 164-177. <https://doi.org/10.1016/j.rser.2014.11.023>
- [5] Ghadikolaee, S. S., M. Yassari, H. Sadeghi, Kh Hosseinzadeh, and D. D. Ganji. "Investigation on thermophysical properties of Tio2–Cu/H2O hybrid nanofluid transport dependent on shape factor in MHD stagnation point flow." *Powder technology* 322 (2017): 428-438. <https://doi.org/10.1016/j.powtec.2017.09.006>
- [6] Aladdin, Nur Adilah Liyana, Norfifah Bachok, and I. Pop. "Cu-Al2O3/water hybrid nanofluid flow over a permeable moving surface in presence of hydromagnetic and suction effects." *Alexandria Engineering Journal* 59, no. 2 (2020): 657-666. <https://doi.org/10.1016/j.aej.2020.01.028>
- [7] Bakar, Shahirah Abu, Norihan Md Arifin, Norfifah Bachok, and Fadzilah Md Ali. "Effect of thermal radiation and MHD on hybrid Ag–TiO2/H2O nanofluid past a permeable porous medium with heat generation." *Case Studies in Thermal Engineering* 28 (2021): 101681. <https://doi.org/10.1016/j.csite.2021.101681>

- [8] Gul, Taza, Kashifullah, M. Bilal, Wajdi Alghamdi, M. Imran Asjad, and Thabet Abdeljawad. "Hybrid nanofluid flow within the conical gap between the cone and the surface of a rotating disk." *Scientific Reports* 11, no. 1 (2021): 1180. <https://doi.org/10.1038/s41598-020-80750-y>
- [9] Hussain, Azad, Ali Hassan, Qasem Al Mdallal, Hijaz Ahmad, Aysha Rehman, Mohamed Altanji, and Mubashar Arshad. "Heat transport investigation of magneto-hydrodynamics (SWCNT-MWCNT) hybrid nanofluid under the thermal radiation regime." *Case Studies in Thermal Engineering* 27 (2021): 101244. <https://doi.org/10.1016/j.csite.2021.101244>
- [10] Lund, Liaquat Ali, Zurni Omar, Sumera Dero, Yuming Chu, and Ilyas Khan. "Temporal stability analysis of magnetized hybrid nanofluid propagating through an unsteady shrinking sheet: Partial slip conditions." *Computers, Materials and Continua* 66, no. 2 (2020): 1963-1975. <https://doi.org/10.32604/cmc.2020.011976>
- [11] Muhammad, Khursheed, T. Hayat, A. Alsaedi, and B. Ahmad. "Melting heat transfer in squeezing flow of basefluid (water), nanofluid (CNTs+ water) and hybrid nanofluid (CNTs+ CuO+ water)." *Journal of Thermal Analysis and Calorimetry* 143 (2021): 1157-1174. <https://doi.org/10.1007/s10973-020-09391-7>
- [12] Rashidi, Mohammad Mehdi, Maryam Sadri, and Mikhail A. Sheremet. "Numerical simulation of hybrid nanofluid mixed convection in a lid-driven square cavity with magnetic field using high-order compact scheme." *Nanomaterials* 11, no. 9 (2021): 2250. <https://doi.org/10.3390/nano11092250>
- [13] Jamshed, Wasim, Nor Ain Azeany Mohd Nasir, Siti Suzilliana Putri Mohamed Isa, Rabia Safdar, Faisal Shahzad, Kottakkaran Sooppy Nisar, Mohamed R. Eid, Abdel-Haleem Abdel-Aty, and I. S. Yahia. "Thermal growth in solar water pump using Prandtl–Eyring hybrid nanofluid: a solar energy application." *Scientific reports* 11, no. 1 (2021): 18704. <https://doi.org/10.1038/s41598-021-98103-8>
- [14] Angstrom, Anders. "Solar and terrestrial radiation. Report to the international commission for solar research on actinometric investigations of solar and atmospheric radiation." *Quarterly Journal of the Royal Meteorological Society* 50, no. 210 (1924): 121-126.
- [15] Qu, Jian, Ruomei Zhang, Zhihao Wang, and Qian Wang. "Photo-thermal conversion properties of hybrid CuO-MWCNT/H₂O nanofluids for direct solar thermal energy harvest." *Applied Thermal Engineering* 147 (2019): 390-398. <https://doi.org/10.1016/j.applthermaleng.2018.10.094>
- [16] Acharya, Nilankush. "On the flow patterns and thermal behaviour of hybrid nanofluid flow inside a microchannel in presence of radiative solar energy." *Journal of Thermal Analysis and Calorimetry* 141 (2020): 1425-1442. <https://doi.org/10.1007/s10973-019-09111-w>
- [17] Alzahrani, Abdullah Khamis, Malik Zaka Ullah, Ali Saleh Alshomrani, and Taza Gul. "Hybrid nanofluid flow in a Darcy-Forchheimer permeable medium over a flat plate due to solar radiation." *Case Studies in Thermal Engineering* 26 (2021): 100955. <https://doi.org/10.1016/j.csite.2021.100955>
- [18] Akilu, Suleiman, Aklilu Tesfamichael Baheta, Mior Azman M. Said, Alina Adriana Minea, and K. V. Sharma. "Properties of glycerol and ethylene glycol mixture based SiO₂-CuO/C hybrid nanofluid for enhanced solar energy transport." *Solar Energy Materials and Solar Cells* 179 (2018): 118-128. <https://doi.org/10.1016/j.solmat.2017.10.027>
- [19] Al-Mahmodi, Akram Fadhl, Lukmon Owolabi Afolabi, Mohammed Ghaleb Awadh, Mohammad Faizal Mohideen Batcha, Nigali Zamani, Norasikin Mat Isa, and Djamal Hissein Didane. "Thermal Behaviour of Nanocomposite Phase Change Material for Solar Thermal Applications." *Journal of Advanced Research in Fluid Mechanics and Thermal Sciences* 88, no. 2 (2021): 133-146.
- [20] Jahan, Sultana, M. Ferdows, M. D. Shamshuddin, and Khairy Zaimi. "Effects of solar radiation and viscous dissipation on mixed convective non-isothermal hybrid nanofluid over moving thin needle." *Journal of Advanced Research in Micro and Nano Engineering* 3, no. 1 (2021): 1-11.
- [21] Rabbi, Hossain Md Fazle, and Ahmet Z. Sahin. "Performance improvement of solar still by using hybrid nanofluids." *Journal of Thermal Analysis and Calorimetry* 143, no. 2 (2021): 1345-1360. <https://doi.org/10.1007/s10973-020-10155-6>
- [22] Saghir, M. Z., and M. M. Rahman. "Forced convection of Al₂O₃-Cu, TiO₂-SiO₂, FWCNT-Fe₃O₄, and ND-Fe₃O₄ hybrid nanofluid in porous media." *Energies* 13, no. 11 (2020): 2902. <https://doi.org/10.3390/en13112902>
- [23] Slimani, Rabeh, Abderrahmane Aissa, Fateh Mebarek-Oudina, Umair Khan, M. Sahnoun, Ali J. Chamkha, and M. A. Medebber. "Natural convection analysis flow of Al₂O₃-Cu/water hybrid nanofluid in a porous conical enclosure subjected to the magnetic field." *The European Physical Journal Applied Physics* 92, no. 1 (2020): 10904. <https://doi.org/10.1051/epjap/2020200260>
- [24] Abu Bakar, Shahirah, Norihan Md Arifin, Najiyah Safwa Khashi'ie, and Norfifah Bachok. "Hybrid nanofluid flow over a permeable shrinking sheet embedded in a porous medium with radiation and slip impacts." *Mathematics* 9, no. 8 (2021): 878. <https://doi.org/10.3390/math9080878>

- [25] Manh, Tran Dinh, I. Tlili, Ahmad Shafee, Trung Nguyen-Thoi, and Hassen Hamouda. "Modeling of hybrid nanofluid behavior within a permeable media involving buoyancy effect." *Physica A: Statistical Mechanics and its Applications* 554 (2020): 123940. <https://doi.org/10.1016/j.physa.2019.123940>
- [26] Lawrence, Jino, and A. Vanav Kumar. "MHD natural convection of hybrid nanofluid in a porous cavity heated with a sinusoidal temperature distribution." *Computational Thermal Sciences: An International Journal* 13, no. 5 (2021). <https://doi.org/10.1615/ComputThermalScien.2021037663>
- [27] Khan, Umair, Aurang Zaib, Sakhinah Abu Bakar, Nepal Chandra Roy, and Anuar Ishak. "Buoyancy effect on the stagnation point flow of a hybrid nanofluid toward a vertical plate in a saturated porous medium." *Case Studies in Thermal Engineering* 27 (2021): 101342. <https://doi.org/10.1016/j.csite.2021.101342>
- [28] Maitra, Shreyasi, Dipak Kumar Mandal, Nirmalendu Biswas, Aparesh Datta, and Nirma K. Manna. "Hydrothermal performance of hybrid nanofluid in a complex wavy porous cavity imposing a magnetic field." *Materials Today: Proceedings* 52 (2022): 419-426. <https://doi.org/10.1016/j.matpr.2021.09.078>
- [29] Shah, Zahir, Anwar Saeed, Imran Khan, Mahmoud M. Selim, Ikramullah, and Poom Kumam. "Numerical modeling on hybrid nanofluid (Fe₃O₄+ MWCNT/H₂O) migration considering MHD effect over a porous cylinder." *Plos one* 16, no. 7 (2021): e0251744. <https://doi.org/10.1371/journal.pone.0251744>
- [30] Ganesh, N. Vishnu, AK Abdul Hakeem, and B. Ganga. "Darcy–Forchheimer flow of hydromagnetic nanofluid over a stretching/shrinking sheet in a thermally stratified porous medium with second order slip, viscous and Ohmic dissipations effects." *Ain Shams Engineering Journal* 9, no. 4 (2018): 939-951. <https://doi.org/10.1016/j.asej.2016.04.019>
- [31] Gul, Taza, Muhammad Bilal, Anwar Saeed, Wajdi Alghamdi, Safyan Mukhtar, Hussam Alrabaiah, and Ebenezer Bonyah. "Viscous dissipated hybrid nanofluid flow with Darcy–Forchheimer and forced convection over a moving thin needle." *AIP Advances* 10, no. 10 (2020). <https://doi.org/10.1063/5.0022210>
- [32] Khan, Sohail A., M. Ijaz Khan, Tasawar Hayat, and Ahmed Alsaedi. "Darcy-Forchheimer hybrid (MoS₂, SiO₂) nanofluid flow with entropy generation." *Computer Methods and Programs in Biomedicine* 185 (2020): 105152. <https://doi.org/10.1016/j.cmpb.2019.105152>
- [33] Ramesh, G. K., S. A. Shehzad, and Mohsen Izadi. "Thermal transport of hybrid liquid over thin needle with heat sink/source and Darcy–Forchheimer porous medium aspects." *Arabian Journal for Science and Engineering* 45, no. 11 (2020): 9569-9578. <https://doi.org/10.1007/s13369-020-04853-4>
- [34] Abu Bakar, Shahirah, Nur Syahirah Wahid, Norihan Md Arifin, and Najiyah Safwa Khashi'ie. "The flow of hybrid nanofluid past a permeable shrinking sheet in a Darcy–Forchheimer porous medium with second-order velocity slip." *Waves in Random and Complex Media* (2022): 1-18. <https://doi.org/10.1080/17455030.2021.2020375>
- [35] Nayan, Asmahani, Nur Izzatie Farhana Ahmad Fauzan, Mohd Rijal Ilias, Shahida Farhan Zakaria, and Noor Hafizah Zainal Aznam. "Aligned magnetohydrodynamics (MHD) flow of hybrid nanofluid over a vertical plate through porous medium." *Journal of Advanced Research in Fluid Mechanics and Thermal Sciences* 92, no. 1 (2022): 51-64.
- [36] Qi, W. Hui, M. P. Wang, and Q. H. Liu. "Shape factor of nonspherical nanoparticles." *Journal of materials science* 40, no. 9-10 (2005): 2737-2739. <https://doi.org/10.1007/s10853-005-2119-0>
- [37] Ghadikolaei, S. S., M. Yassari, H. Sadeghi, Kh Hosseinzadeh, and D. D. Ganji. "Investigation on thermophysical properties of TiO₂–Cu/H₂O hybrid nanofluid transport dependent on shape factor in MHD stagnation point flow." *Powder technology* 322 (2017): 428-438. <https://doi.org/10.1016/j.powtec.2017.09.006>
- [38] Khan, M., J. Ahmed, F. Sultana, and M. Sarfraz. "Non-axisymmetric Homann MHD stagnation point flow of Al₂O₃-Cu/water hybrid nanofluid with shape factor impact." *Applied Mathematics and Mechanics* 41 (2020): 1125-1138. <https://doi.org/10.1007/s10483-020-2638-6>
- [39] Gholinia, M., SAH Kiaeian Moosavi, M. Pourfallah, S. Gholinia, and D. D. Ganji. "A numerical treatment of the TiO₂/C₂H₆O₂–H₂O hybrid base nanofluid inside a porous cavity under the impact of shape factor in MHD flow." *International Journal of Ambient Energy* 42, no. 16 (2021): 1815-1822. <https://doi.org/10.1080/01430750.2019.1614996>
- [40] Benkhedda, Mohammed, Toufik Boufendi, Tahar Tayebi, and Ali J. Chamkha. "Convective heat transfer performance of hybrid nanofluid in a horizontal pipe considering nanoparticles shapes effect." *Journal of Thermal analysis and Calorimetry* 140, no. 1 (2020): 411-425. <https://doi.org/10.1007/s10973-019-08836-y>
- [41] Chu, Yu-Ming, Kottakkaran Sooppy Nisar, Umair Khan, Hamed Daei Kasmaei, Manuel Malaver, Aurang Zaib, and Ilyas Khan. "Mixed convection in MHD water-based molybdenum disulfide-graphene oxide hybrid nanofluid through an upright cylinder with shape factor." *Water* 12, no. 6 (2020): 1723. <https://doi.org/10.3390/w12061723>
- [42] Dinarvand, Saeed, and Mohammadreza Nademi Rostami. "Three-dimensional squeezed flow of aqueous magnetite–graphene oxide hybrid nanofluid: a novel hybridity model with analysis of shape factor effects." *Proceedings of the Institution of Mechanical Engineers, Part E: Journal of Process Mechanical Engineering* 234, no. 2 (2020): 193-205. <https://doi.org/10.1177/2F0954408920906274>

- [43] Anwar, Talha, Poom Kumam, and Phatiphat Thounthong. "A comparative fractional study to evaluate thermal performance of NaAl₃-MoS₂-Co hybrid nanofluid subject to shape factor and dual ramped conditions." *Alexandria Engineering Journal* 61, no. 3 (2022): 2166-2187. <https://doi.org/10.1016/j.aej.2021.06.085>
- [44] Hafeez, Muhammad, Rai Sajjad, and Hashim. "Heat transfer attributes of MoS₂/Al₂O₃ hybrid nanomaterial flow through converging/diverging channels with shape factor effect." *Advances in Mechanical Engineering* 13, no. 5 (2021): 16878140211021289. <https://doi.org/10.1177%2F16878140211021289>
- [45] Khan, Umair, Aurang Zaib, Ioan Pop, Sakhinah Abu Bakar, and Anuar Ishak. "Stagnation point flow of a micropolar fluid filled with hybrid nanoparticles by considering various base fluids and nanoparticle shape factors." *International Journal of Numerical Methods for Heat & Fluid Flow* 32, no. 7 (2022): 2320-2344. <https://doi.org/10.1108/HFF-07-2021-0445>
- [46] Khashi'ie, Najiyah Safwa, Norihan Md Arifin, Mikhail Sheremet, and Ioan Pop. "Shape factor effect of radiative Cu-Al₂O₃/H₂O hybrid nanofluid flow towards an EMHD plate." *Case Studies in Thermal Engineering* 26 (2021): 101199. <https://doi.org/10.1016/j.csite.2021.101199>
- [47] Rekha Sahoo, Rashmi. "Effect of various shape and nanoparticle concentration based ternary hybrid nanofluid coolant on the thermal performance for automotive radiator." *Heat and Mass Transfer* 57, no. 5 (2021): 873-887. <https://doi.org/10.1007/s00231-020-02971-1>
- [48] Khan, M. Ijaz, and Faris Alzahrani. "Free convection and radiation effects in nanofluid (Silicon dioxide and Molybdenum disulfide) with second order velocity slip, entropy generation, Darcy-Forchheimer porous medium." *International Journal of Hydrogen Energy* 46, no. 1 (2021): 1362-1369. <https://doi.org/10.1016/j.ijhydene.2020.09.240>
- [49] Xie, Hongmei, Bin Jiang, Bo Liu, Qinghang Wang, Junyao Xu, and Fusheng Pan. "An investigation on the tribological performances of the SiO₂/MoS₂ hybrid nanofluids for magnesium alloy-steel contacts." *Nanoscale research letters* 11 (2016): 1-17. <https://doi.org/10.1186/s11671-016-1546-y>
- [50] Takabi, Behrouz, and Saeed Salehi. "Augmentation of the heat transfer performance of a sinusoidal corrugated enclosure by employing hybrid nanofluid." *Advances in Mechanical Engineering* 6 (2014): 147059. <https://doi.org/10.1155%2F2014%2F147059>
- [51] Ghalambaz, Mohammad, S. A. M. Mehryan, Ahmad Hajjar, and Ali Veismoradi. "Unsteady natural convection flow of a suspension comprising Nano-Encapsulated Phase Change Materials (NEPCMs) in a porous medium." *Advanced Powder Technology* 31, no. 3 (2020): 954-966. <https://doi.org/10.1016/j.apt.2019.12.010>
- [52] Dinarvand, Saeed, Seyed Mehdi Mousavi, Mohammad Yousefi, and Mohammadreza Nademi Rostami. "MHD flow of MgO-Ag/water hybrid nanofluid past a moving slim needle considering dual solutions: An applicable model for hot-wire anemometer analysis." *International Journal of Numerical Methods for Heat & Fluid Flow* 32, no. 2 (2022): 488-510. <https://doi.org/10.1108/HFF-01-2021-0042>
- [53] Mansourian, Mahdi, Saeed Dinarvand, and Ioan Pop. "Aqua cobalt ferrite/Mn-Zn ferrite hybrid nanofluid flow over a nonlinearly stretching permeable sheet in a porous medium." *Journal of Nanofluids* 11, no. 3 (2022): 383-391. <https://doi.org/10.1166/jon.2022.1841>
- [54] Aly, Emad H., and Ioan Pop. "MHD flow and heat transfer over a permeable stretching/shrinking sheet in a hybrid nanofluid with a convective boundary condition." *International Journal of Numerical Methods for Heat & Fluid Flow* 29, no. 9 (2019): 3012-3038. <https://doi.org/10.1108/HFF-12-2018-0794>
- [55] Reddy Gorla, Rama Subba, and Ibrahim Sidawi. "Free convection on a vertical stretching surface with suction and blowing." *Applied Scientific Research* 52 (1994): 247-257. <https://doi.org/10.1007/BF00853952>
- [56] Ismail, Nurul Syuhada, Norihan Md Arifin, Roslinda Nazar, and Norfifah Bachok. "Stability analysis of unsteady MHD stagnation point flow and heat transfer over a shrinking sheet in the presence of viscous dissipation." *Chinese journal of physics* 57 (2019): 116-126. <https://doi.org/10.1016/j.ciph.2018.12.005>
- [57] Ismail, N. S., S. S. P. M. Isa, N. M. Arifin, R. Nazar, and N. Bachok. "The Effect of Thermal Radiation, Velocity Slip And Viscous Dissipation On Mhd Stagnation-Point Flow And Heat Transfer Over A Shrinking Sheet In Nanofluids With Stability Analysis." *Magneto hydrodynamics (0024-998X)* 57, no. 3 (2021). <https://doi.org/10.22364/mhd.57.3.3>
- [58] Weidman, P. D., D. G. Kubitschek, and A. M. J. Davis. "The effect of transpiration on self-similar boundary layer flow over moving surfaces." *International journal of engineering science* 44, no. 11-12 (2006): 730-737. <https://doi.org/10.1016/j.ijengsci.2006.04.005>
- [59] Merkin, J. H. "On dual solutions occurring in mixed convection in a porous medium." *Journal of engineering Mathematics* 20, no. 2 (1986): 171-179. <https://doi.org/10.1007/bf00042775>
- [60] Abu Bakar, Shahirah, Norihan Md Arifin, Fadzilah Md Ali, Norfifah Bachok, Roslinda Nazar, and Ioan Pop. "A stability analysis on mixed convection boundary layer flow along a permeable vertical cylinder in a porous medium filled with a nanofluid and thermal radiation." *Applied Sciences* 8, no. 4 (2018): 483. <https://doi.org/10.3390/app8040483>

- [61] Bakar, Shahirah Abu, Norihan Md Arifin, Roslinda Nazar, Fadzilah Md Ali, Norfifah Bachok, and Ioan Pop. "The effects of suction on forced convection boundary layer stagnation point slip flow in a darcy porous medium towards a shrinking sheet with presence of thermal radiation: A stability analysis." *Journal of Porous Media* 21, no. 7 (2018). <https://doi.org/10.1615/JPorMedia.2018019722>
- [62] Ismail, N. S., N. M. Ariffin, R. Nazar, and N. Bachok. "Stability analysis of stagnation-point flow and heat transfer over an exponentially shrinking sheet with heat generation." *Malaysian Journal of Mathematical Sciences* 13, no. 2 (2019): 107-122.
- [63] Harris, S. D., D. B. Ingham, and I. Pop. "Mixed convection boundary-layer flow near the stagnation point on a vertical surface in a porous medium: Brinkman model with slip." *Transport in Porous Media* 77 (2009): 267-285. <https://doi.org/10.1007/s11242-008-9309-6>